

OPTICS,
QUANTUM ELECTRONICS

Quick Ellipsometric Technique for Determining the Thicknesses and Optical Constant Profiles of Fe/SiO₂/Si(100) Nanostructures during Growth

I. A. Tarasov^{*a, b}, N. N. Kosyrev^{a, b}, S. N. Varnakov^{a, b}, S. G. Ovchinnikov^a,
S. M. Zharkov^{a, d}, V. A. Shvets^{c, e}, S. G. Bondarenko^a, and O. E. Tereshchenko^c

^a Kirenskii Institute of Physics, Siberian Branch, Russian Academy of Sciences, Akademgorodok,
Krasnoyarsk, 660036 Russia

*e-mail: tia@iph.krasn.ru

^b Reshetnev Siberian State Aerospace University, pr. im. Gazety “Krasnoyarskii Rabochii” 31, Krasnoyarsk, 660014 Russia

^c Institute of Semiconductor Physics, Siberian Branch, Russian Academy of Sciences, pr. Akademika Lavrent’eva 13,
Novosibirsk, 630090 Russia

^d Siberian Federal University, Svobodnyi pr. 79, Krasnoyarsk, 660041 Russia

^e Novosibirsk State University, ul. Pirogova 2, Novosibirsk, 630090 Russia

Received October 4, 2011

Abstract—An algorithm is developed to perform rapid control of the thickness and optical constants of a film structure during growth. This algorithm is tested on Fe/SiO₂/Si(100) structures grown in an Angara molecular-beam epitaxy setup. The film thicknesses determined during their growth are compared with X-ray spectral fluorescence analysis and transmission electron microscopy data.

DOI: 10.1134/S1063784212090241

Studying thin magnetic metal films on semiconductor substrates is now of particular interest due to new physical properties of these structures and the prospects of their application in spintronics [1–3]. The film thicknesses in those works were varied from several fractions of a nanometer to tens of nanometers. The technological growth parameters are usually chosen using preliminary calibrations, which can substantially change during growth. Therefore, it is necessary to control the layer thickness in such a structure during growth.

The experimental techniques most widely used to perform in situ film thickness control during growth are as follows: thickness measurement from the difference between beats in a quartz resonator, the high-energy electron diffraction, and ellipsometry. To obtain reliable film thicknesses using a quartz resonator, it should be located as close as possible to a synthesis region and should be thermally stabilized, which requires an additional complication of the experimental technique. Moreover, this method is inconvenient during the formation of multicomponent systems. The diffraction of fast electrons can be used to calculate the coating thickness from specular reflection oscillations during layer-by-layer growth of epitaxial films [4] and cannot be used for thickness measurements during the formation of polycrystalline and amorphous structures.

Among these methods, ellipsometry is a sensitive method that can almost continuously obtain information on the processes occurring on the surface of a growing sample without affecting its structure. Apart from thickness, an ellipsometric experiment can also give information on the optical properties, in particular, the depth profiles of optical constants in a nonuniform layer [5–9]. Modern fast ellipsometers can maintain an almost continuous ellipsometric data flow measured during growth, which opens up fresh opportunities for solving the inverse problem of ellipsometry in a nondestructive manner. This problem can rather easily be solved when the thickness dependence of the ellipsometric parameters is known [8]. In a real experiment, however, the ellipsometric parameters are measured during growth as functions of time and can only roughly be estimated if the growth rate is calibrated.

Shvets [9] considered the problem of restoring optical constant profiles from a “growth curve,” namely, the ellipsometric parameters measured during the growth of a nonuniform layer. He proposed an algorithm to determine these profiles, which achieved good results provided the gradient of the optical constants is small, $G = \lambda |dN/dz| \ll 1$, where $N = n - ik$ is the complex refractive index and λ is the wavelength. This algorithm is based on the relative derivatives of the ellipsometric parameters determined experimentally from the growth curve at a high density of measured points. For the reverse inequality ($G \gg 1$), gen-

erally speaking this problem has no unambiguous solution. The physical cause of the ambiguity consists in the fact that the role of interference in the formation of an ellipsometric response increases with the optical constant gradient.

Thus, when ellipsometric data are interpreted, problems appear in solving the inverse problem [10], i.e., in choosing an adequate optical model for a grown structure that can describe it at an acceptable accuracy [11].

Nevertheless, for experimental data to be preliminarily interpreted during film growth, it is sufficient to use an algorithm with a simple optical model to perform real-time estimation of the thickness and optical constants of a growing film. The purpose of this work is to develop such a rapid technique to control the physical characteristics of a structure during an experiment.

During ellipsometric measurements, researchers determine the ratio of complex reflection coefficients R_p and R_s ,

$$\rho = \frac{R_p}{R_s} = \tan \psi e^{i\Delta}, \quad (1)$$

where

$$\tan \psi = \frac{|R_p|}{|R_s|},$$

$$\Delta = \arg \frac{R_p}{R_s}.$$

Angles ψ and Δ are called the ellipsometric parameters of a reflecting system and are measured during an ellipsometric experiment. Quantity ρ is the complex ellipsometric parameter, and Eq. (1) is called the basic ellipsometry equation [10].

The rapid technique of solving the inverse ellipsometry problem developed in this work is based on the numerical Newton's iteration method extended to the complex variable region [12].

If the ratio of the reflection coefficients is designated as g , the inverse ellipsometry problem can be considered as the problem of searching for the values of N_a , N_i , φ , d_j , and λ for which the function

$$f = g - \tan \psi e^{i\Delta} \quad (2)$$

vanishes. Here, we have

$$g = \frac{R_p}{R_s}, \quad (3)$$

where R_p and R_s are the calculated complex reflection coefficients for a multilayer structure; N_a is the complex refractive index of the medium; N_j and d_j are the complex refractive index and the thickness of the j th layer, respectively; φ is the angle of radiation incidence on the structure; and λ is the wavelength.

In Eq. (3), the reflection coefficients for the p and s components of incident radiation ($R_{p,s}$) can be found

for any number of layers from the recurrent relationship

$$R_{j+1} = \frac{r_{j+1}(1 - r_{j+1}R_j) + (R_j - r_{j+1})X_{j+1}}{1 - r_{j+1}R_j + r_{j+1}(R_j - r_{j+1})X_{j+1}}, \quad (4)$$

where

$$X_{j+1} = e^{-2i\delta_{j+1}}, \quad \delta_{j+1} = 2\pi \frac{d_{j+1}}{\lambda} \sqrt{N_{j+1}^2 - \sin^2 \varphi}. \quad (5)$$

In Eq. (4), r_{j+1} are the Fresnel coefficients for the j th + 1 layer reduced to the external medium and X_{j+1} is the exponential function of the phase thickness for the j th + 1 layer.

Using this function, we developed an algorithm to monitor the growth of an Fe/SiO₂/Si(100) structure and to perform real-time calculations of d_{Fe} , n_{Fe} , and k_{Fe} for each pair of experimentally obtained ψ and Δ .

Given an approximate value of root x_0 of function $f(x)$ in Newton's method, more exact value x_1 is determined as

$$x_1 = x_0 - \frac{f(x_0)}{|df/dx|_{x=x_0}}. \quad (6)$$

Accordingly, a more exact iron film thickness in this algorithm is

$$d_1 = d_0 - \frac{f(d_0)}{|df/dd|_{d=d_0}}, \quad (7)$$

where the subscript of d is the number of approximation.

During film growth, an array of ellipsometric angles ψ and Δ is measured. The algorithm of calculating the profiles of the optical constants is as follows. The first pair of ψ and Δ is chosen from the data array, and the first approximation of the quantity to be determined (in this case, d) is specified for this pair. The optical parameters of the film are set as functions of a sputtered substance [13], and the ratios of the reflection coefficients are calculated for the zeroth approximation. The condition of the end of iterations for searching for the root is set as

$$|d_{k+1} - d_k| < \varepsilon \Rightarrow d^{(*)} \approx d_{k+1}, \quad (8)$$

$$k = 0, 1, 2, 3 \dots n,$$

where $d^{(*)}$ is the root of Eq. (1). The root corresponding to the minimum modulus of complex function f is then chosen. This fact is the principal difference from Newton's method [12], where d_{k+1} is the desired root.

Then, refractive index n is calculated for the obtained thickness and extinction coefficient k is calculated for new d and n . Obtained roots d , n , and k are the zeroth approximation for the next pair of experimental values of ψ and Δ . The calculation according to this scheme continues until d , n , and k are calculated for each pair of ψ and Δ . Using the obtained values of d , n , and k , we calculate the values of ψ and Δ and the

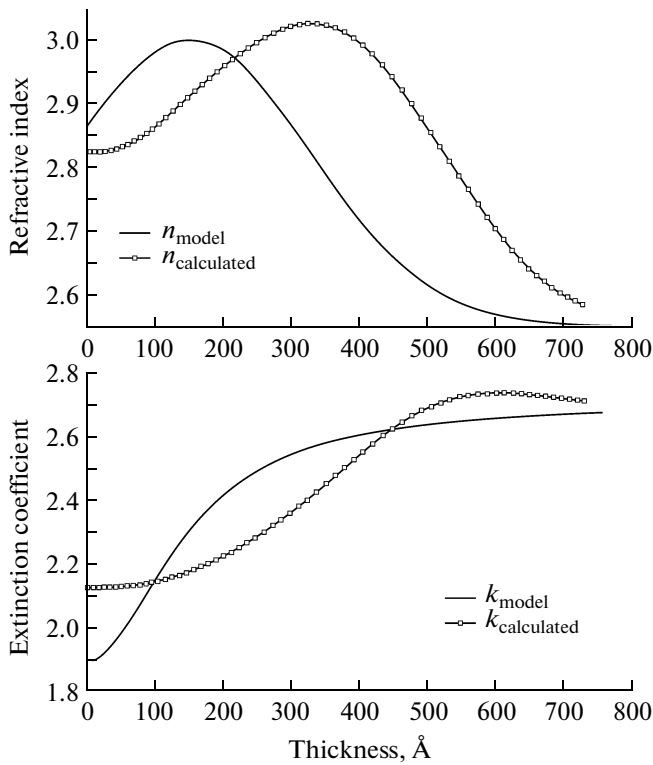


Fig. 1. Model and restored profiles of the optical constants of a film growing in a numerical experiment.

minimization function is found by the well-known formula [10]

$$\sigma = \frac{1}{M} \left\{ \sum_{j=1}^M \left((\Delta_{\text{ex}}^j - \Delta_{\text{calc}}^j)^2 + (\psi_{\text{ex}}^j - \psi_{\text{calc}}^j)^2 \right) \right\}. \quad (9)$$

After the calculation, the calculated results are presented in a graphical form.

To test the developed algorithms, we performed a numerical experiment in which film growth with variable optical parameters was simulated. The dependences of the refractive index and extinction coefficient on the model structure thickness during growth were set in an arbitrary form. The direct problem was then solved and the dependences of ellipsometric parameters ψ and Δ on the growth time were calculated. The developed algorithm was then used to restore n and k profiles (Fig. 1) and the dependence of the film thickness on the growth time (Fig. 2). When analyzing the calculated data, we found that the error of determining the film thickness by this algorithm is several percent. It should be noted, however, that the restored profiles of the refractive index and extinction coefficient only qualitatively reflect the initial depth profiles. When a structure grows, the distribution of its optical constants is affected by the structural characteristics, the imperfection of growing layers, the presence of foreign inclusions, and so on. Therefore, a qualitative depth profile of the optical constants rather

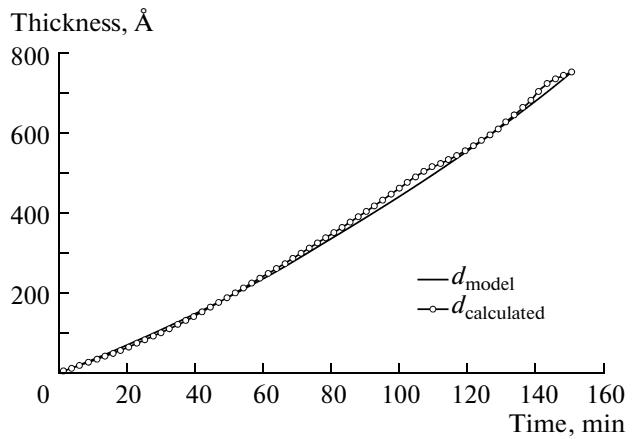


Fig. 2. Initial and restored dependences of the model film thickness on the growth time.

than an exact depth profile is important to perform real-time analysis of film growth.

Experimental testing of the rapid technique of determining the optical parameters and the film thickness was performed on a series of thin-film Fe/SiO₂ structures on single-crystal Si(100) substrates with various silicon dioxide and iron layer thicknesses. Iron films were formed by thermal evaporation in the ultra-high-vacuum chamber of an Angara setup at room temperature of the substrate [14]. Ellipsometric measurements were carried out with an LEF-751M laser ellipsometer [15].

The calculation was performed using a two-layer model. The first layer consisted of silicon dioxide SiO₂, whose thickness was calculated from the ellipsometric data obtained before the beginning of evaporation using the well-known data for silicon dioxide ($n_{\text{SiO}_2} = 1.456$, $k_{\text{SiO}_2} = 0$ [16]). The second layer consisted of a growing iron film for which parameters d_{Fe} , n_{Fe} , and k_{Fe} were calculated. The refractive index and extinction coefficient of the silicon Si(100) substrate were $n_{\text{Si}} = 3.865$ and $k_{\text{Si}} = 0.023$, respectively.

Figure 3 shows the results of calculation by the developed technique for an Fe/SiO₂/Si(100) sample. The calculated Fe film thickness is 490 Å, which agrees well with the X-ray fluorescence (XRF) analysis data in [17] ($d_{\text{Fe}} = 492$ Å). The calculated optical constants for the formed Fe film ($n_{\text{Fe}} = 2.82$, $k_{\text{Fe}} = 2.86$) differ from the refractive index and extinction coefficient of bulk Fe determined in [13] by at most 2%.

The optical constant curves can be conventionally divided into the following three characteristic regions (Fig. 3). In region *AB*, the optical indices of the Fe film increase sharply. In this case, we deal with the island growth of polycrystalline iron [18], and the probing beam is reflected from the growing surface and contains information on reflection from both deposited islands and the substrate surface. This mode continues

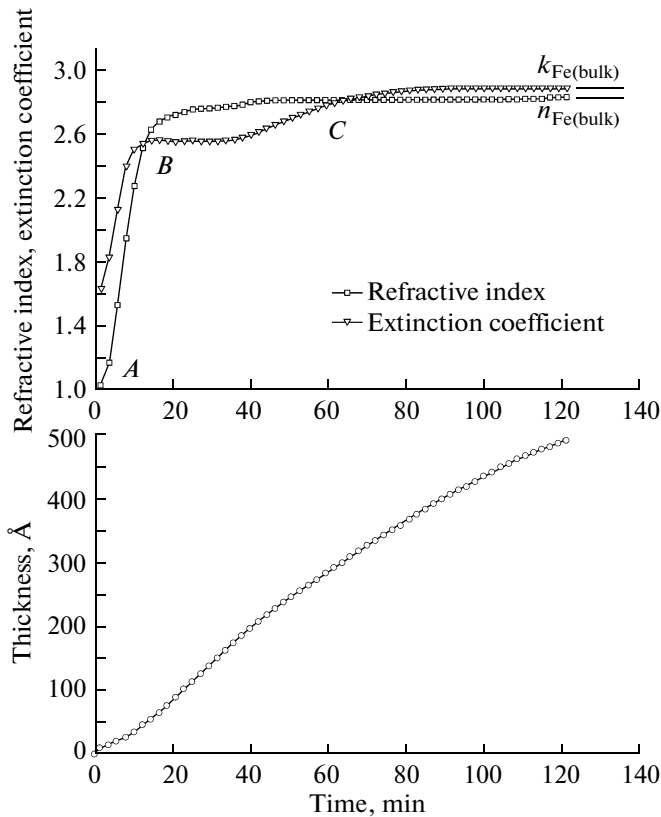


Fig. 3. Control of the changes in refractive index n , extinction coefficient k , and thickness d during Fe film growth.

up to the formation of a continuous iron layer. Thus, point *B* (Fe thickness of ~ 50 Å) can correspond to the formation of a continuous iron layer.

Region *BC* corresponds to the growth of a continuous homogeneous iron film, and the effect of the $\text{SiO}_2/\text{Si}(100)$ substrate on the refractive index and the extinction coefficient is substantial. At point *C* (Fe thickness of ~ 370 Å), this effect weakens because of high absorption in iron, and the refractive index and extinction coefficient reach the values of bulk Fe and remain unchanged during further growth.

Comparison of the calculated thicknesses and XSF data

Sample no.	Calculated thickness d , Å	Minimization function $\sigma \times 10^{-3}$	XSF Fe thickness d_{Fe} , Å
1	490	1.41	492
2	142	1.90	146
3	113	2.61	113
4	67	0.24	65
5	52	0.25	50
6	58	0.31	55
7	25	3.90	22

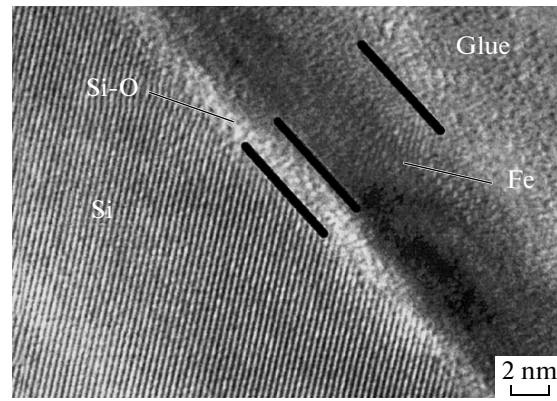


Fig. 4. Electron-microscopic image of the cross section of sample 5.

The calculated iron film thicknesses in comparison with the XSF results are given in the table. An analysis of these data demonstrates that the Fe film thicknesses coincide within the limits of experimental XSF and ellipsometry errors.

To support the XSF data, we carried out electron-microscopic investigations of the cross section of sample 5 (Fig. 4). The amorphous SiO_2 layer thickness is 15 Å and the Fe layer thickness is 50 Å, which also coincides with the XSF data within the limits of experimental error (see the table).

Thus, we developed and tested a rapid technique for determining the optical characteristics and thickness of iron films from one-wavelength ellipsometry data, and the algorithm operation speed allowed us to perform real-time estimation of the physical parameters of a growing film. This technique is sensitive to the first approximation of the optical constants specified at the beginning of calculations.

ACKNOWLEDGMENTS

This work was supported by Integration Project no. 22 of the Siberian and Far East Branches, Russian Academy of Sciences; a program of the Presidium of the Russian Academy of Sciences (project no. 27), the Federal Target Program “Human Capital for Science and Education in Innovative Russia” for 2009–2013, and the program “Spintronics” (project no. 4) of the Department of Physical Sciences, Russian Academy of Sciences.

REFERENCES

1. M. V. Gomoyunova, G. S. Grebenyuk, I. I. Pronin, et al., *Phys. Solid State* **53**, 606 (2011).
2. S. R. Naik, S. Rai, et al., *J. Phys. D: Appl. Phys.* **41**, 115307 (2008).
3. S. N. Varnakov, S. G. Ovchinnikov, J. Bartolomé, et al., *J. Solid State Phenomena* **168–169**, 277 (2011).

4. K. Oura, V. G. Lifshits, A. A. Saranin, et al., *Surface Science: An Introduction* (Springer, Berlin–Heidelberg, 2003).
5. J. C. Charmet and P. G. de Gennes, *J. Opt. Soc. Am.* **73**, 1777 (1983).
6. V. A. Shvets, V. Yu. Prokop'ev, S. I. Chikichev, and N. A. Aul'chenko, *Avtometriya* **43** (5), 71 (2007).
7. T. P. Chen, Y. Liu, M. S. Tse, P. F. Ho, G. Dong, and S. Fung, *Appl. Phys. Lett.* **81**, 4724 (2002).
8. E. E. Dagman, R. I. Lyubinskaya, A. S. Mardezhov, K. K. Svitashov, A. I. Semenenko, and V. A. Shvets, *Ukr. Fiz. Zh.* **29**, 187 (1984).
9. V. A. Shvets, *Avtometriya*, No. 6, 25 (1993).
10. R. M. A. Azzam and N. M. Bashara, *Ellipsometry and Polarized Light* (North Holland, New York, 1977).
11. N. N. Kosyrev, V. N. Zabluda, S. N. Varnakov, et al., *Zh. Strukt. Khim.* **51**, 104 (2010).
12. J. H. Mathews and K. D. Fink, *Numerical Methods. Using Matlab* (Prentice Hall, Jersey, 2001).
13. P. B. Johnson and R. W. Christy, *Phys. Rev. B* **9**, 5056 (1974).
14. S. N. Varnakov, A. A. Lapeshev, S. G. Ovchinnikov, et al., *Prib. Tekh. Eksp.*, No. 6, 125 (2004).
15. E. V. Spesivtsev, S. V. Rykhlytskii, and V. A. Shvets, "Ellipsometer" RF Patent No. 2302623, *Byull. Izobret.* No. 19.
16. *Handbook of Optical Constants of Solids*, Ed. by E. D. Palik (Elsevier, 1998).
17. G. V. Bondarenko, Preprint IFSO-16F (Institute of Physics, Siberian Division, Russian Academy of Sciences, Krasnoyarsk, 1974), p. 40.
18. S. N. Varnakov, I. A. Yakovlev, S. A. Lyashchenko, et al., *Vestn. Sibirsk. Gos. Aerokosm. Univ.* **30**, 45 (2010).

Translated by K. Shakhlevich